FREYA studies of angular momentum in fission

Ramona Vogt (LLNL & UC Davis)

J. Randrup (LBNL)

LLNL-PRES-817210

This work performed under the auspices of the U.S. Department of Energy by
Lawrence Livermore National Laboratory under Contract DE-AC52-07NA27344

FREYA is ideal for studying spin effects in fission

- Angular momentum has been a hot topic in fission for more than 60 years
- Fission fragments typically carry 5-7$\hbar$ approximately directed perpendicular to the fission axis
- The two fragment spins are nearly uncorrelated
- Fragment rotation:
  - causes neutron emission to be anisotropic;
  - influences photon emission;
  - affects searches for novel effects like scission neutrons
- Because FREYA conserves energy and linear & angular momentum, it can elucidate the influence of angular momentum in fission
- We study the influence of the overall angular momentum and those of the fragments on a variety of fission observables

Start from the rotating compound nucleus generated by the incoming neutron

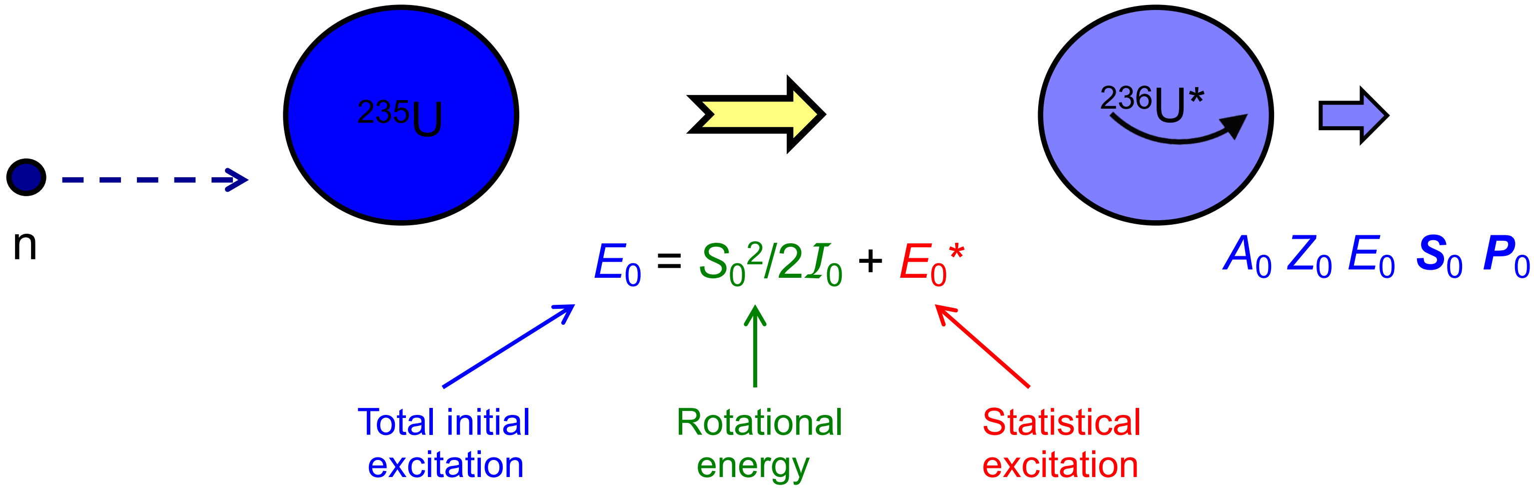

The plane of rotation is determined by the impact parameter of incident neutron; the plane may change due to *pre-fission neutron evaporation* (which is treated the same as the post-fission neutron evaporation from the rotating fragments)

The fragment spins are determined at scission

Average:
Rigid rotation:

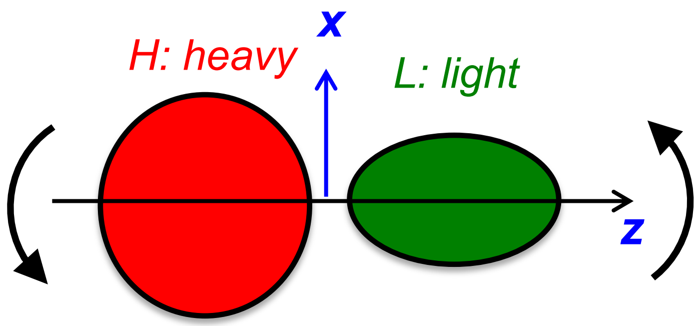

$\left\{ \begin{array}{l} \boldsymbol{z} = \boldsymbol{R}/R \\ \boldsymbol{y} = \boldsymbol{S}_0/S_0 \\ \boldsymbol{x} = \boldsymbol{y} \times \boldsymbol{z} \end{array} \right.$

Individual fragments: $\underline{\boldsymbol{S}}_\mathrm{L} = (\mathcal{I}_\mathrm{L}/\mathcal{I}_\mathrm{tot})\ \boldsymbol{S}_0 \quad \underline{\boldsymbol{S}}_\mathrm{H} = (\mathcal{I}_\mathrm{H}/\mathcal{I}_\mathrm{tot})\ \boldsymbol{S}_0$

Relative motion: $\underline{\boldsymbol{L}} = (\mathcal{I}_\mathrm{rel}/\mathcal{I}_\mathrm{tot})\ \boldsymbol{S}_0 = \boldsymbol{R} \times \boldsymbol{P}$

Conservation:

$\underline{\boldsymbol{S}}_\mathrm{L} + \underline{\boldsymbol{S}}_\mathrm{H} + \underline{\boldsymbol{L}} = \boldsymbol{S}_0$

Fluctuations:
Wriggling & bending

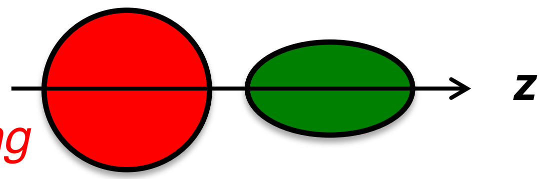

$\boldsymbol{s}_\pm = (s_\pm^x, s_\pm^y, 0)$:
$P(\boldsymbol{s}_\pm) \sim \exp(-\boldsymbol{s}_\pm^2/2\mathcal{I}_\pm T_\mathrm{S})$
Spin temperature: $T_\mathrm{S} = c_\mathrm{S} T_\mathrm{sciss}$

Fluctuations in fragment spin: $\delta S_\mathrm{L}^k = (\mathcal{I}_\mathrm{L}/\mathcal{I}_+)\ s_+^k + s_-^k \quad \delta S_\mathrm{H}^k = (\mathcal{I}_\mathrm{H}/\mathcal{I}_+)\ s_+^k - s_-^k$

Modifications in spin: $\boldsymbol{S}_\mathrm{L} = \underline{\boldsymbol{S}}_\mathrm{L} + \delta\boldsymbol{S}_\mathrm{L} \quad \boldsymbol{S}_\mathrm{H} = \underline{\boldsymbol{S}}_\mathrm{H} + \delta\boldsymbol{S}_\mathrm{H} \quad \boldsymbol{L} = \underline{\boldsymbol{L}} - \delta\boldsymbol{S}_\mathrm{L} - \delta\boldsymbol{S}_\mathrm{H}$

Average rotational energy (rigid): $\underline{E}_\mathrm{rot} = \underline{\boldsymbol{S}}_\mathrm{L}^2/2\mathcal{I}_\mathrm{L} + \underline{\boldsymbol{S}}_\mathrm{H}^2/2\mathcal{I}_\mathrm{H} + \underline{\boldsymbol{L}}^2/2\mathcal{I}_\mathrm{rel} = \boldsymbol{S}_0^2/2\mathcal{I}_\mathrm{tot}$

Total rotational energy (with fluctuations):
Fragment spins dominated by fluctuations!

$E_\mathrm{rot} = \boldsymbol{S}_\mathrm{L}^2/2\mathcal{I}_\mathrm{L} + \boldsymbol{S}_\mathrm{H}^2/2\mathcal{I}_\mathrm{H} + \boldsymbol{L}^2/2\mathcal{I}_\mathrm{rel}$
$= \underline{E}_\mathrm{rot} + \boldsymbol{s}_+^2/2\mathcal{I}_+ + \boldsymbol{s}_-^2/2\mathcal{I}_-$

Neutron evaporation from rotating fragments

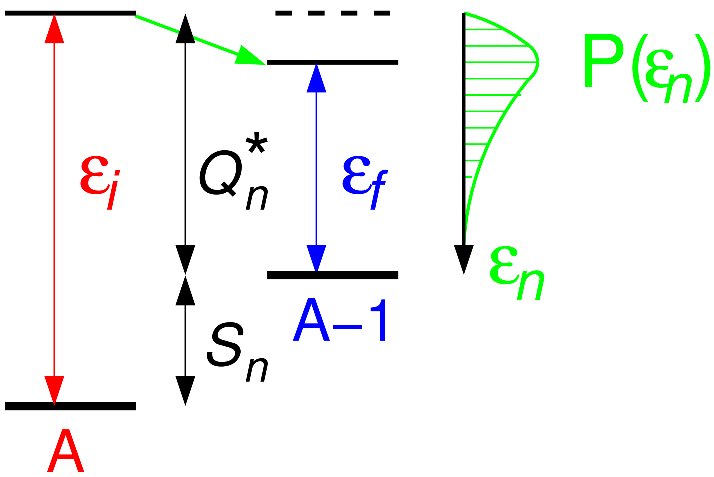

$$M_i^* = M_i^\mathrm{gs} + \varepsilon_i \qquad M_f^* = M_f^\mathrm{gs} + \varepsilon_f \qquad M_i^* = M_f^* + m_\mathrm{n} + \epsilon$$

$$Q_\mathrm{n} \equiv Q_\mathrm{n}^*(\varepsilon_i{=}0) = M_i^\mathrm{gs} - M_f^\mathrm{gs} - m_\mathrm{n} = -S_\mathrm{n}$$

$$Q_\mathrm{n}^* = \varepsilon_i + Q_\mathrm{n} = \varepsilon_i - S_\mathrm{n}$$

$$\epsilon + \varepsilon_f = M_i^* - M_f^\mathrm{gs} - m_\mathrm{n} = Q_\mathrm{n}^* = \begin{cases} \varepsilon_f^\mathrm{max} \\ \epsilon^\mathrm{max} \end{cases}$$

$$T_f^\mathrm{max} = \sqrt{\varepsilon_f^\mathrm{max}/a_f} = \sqrt{Q_\mathrm{n}^*/a_f}$$

Weisskopf-Ewing neutron energy spectrum: $d^3\boldsymbol{p} \sim \sqrt{\epsilon}\, d\epsilon\, d\Omega$ *(non-relativistic)*

$$\frac{d^3N}{d^3\boldsymbol{p}} d^3\boldsymbol{p} \sim \sqrt{\epsilon}\, \mathrm{e}^{-\epsilon/T_f^\mathrm{max}} \sqrt{\epsilon}\, d\epsilon\, d\Omega = \mathrm{e}^{-\epsilon/T_f^\mathrm{max}} \epsilon\, d\epsilon\, d\Omega$$

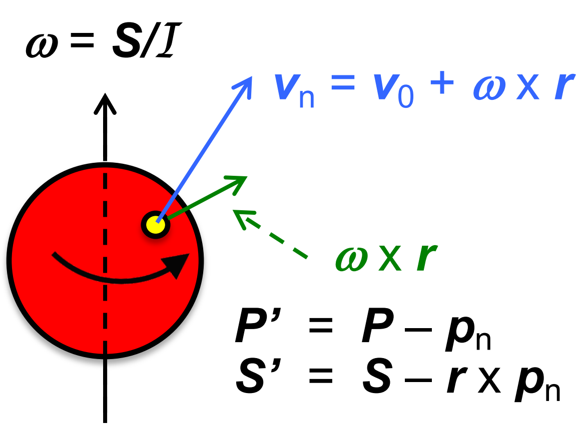

When fragment is rotating, emission from moving surface, v_0, is boosted by local rotational velocity $\boldsymbol{\omega} \times \boldsymbol{r}$ and daughter nucleus absorbs recoil linear and angular momentum

Emission from rotating fragment gives neutron centrifugal boost, resulting in bulge in equatorial plane

Neutron and daughter nucleus Lorentz boosted from emitter frame to laboratory frame

Neutron evaporation conserves energy, linear & angular momentum

Photon emission follows neutron emission

Neutron evaporation has ceases when $E^* < S_n$ (neutron separation energy); the remaining excitation energy is disposed of by sequential photon emission …

… first by statistical photon cascades down to the yrast line …

$$\frac{d^3N}{d^3\mathbf{p}_\gamma} d^3\mathbf{p}_\gamma \sim \left[\frac{\Gamma^2_{\rm GDR}\epsilon^2}{(\epsilon^2-\epsilon_{\rm GDR^2})^2+\Gamma^2_{\rm GDR}\epsilon^2}\right]\epsilon^2 e^{-\epsilon/T_i} \quad \Leftarrow \quad d^3\boldsymbol{p}_\gamma \sim \epsilon^2 d\epsilon\, d\Omega$$

(ultrarelativistic)

$S_f = S_i - 1$

$$E^*_f = E^*_i - \epsilon_\gamma \qquad \epsilon_{\rm GDR} = \left(31.2A^{-1/3} + 20.6A^{-1/6}\right)\,{\rm MeV} \qquad \Gamma_{\rm GDR} = 5\,{\rm MeV}$$

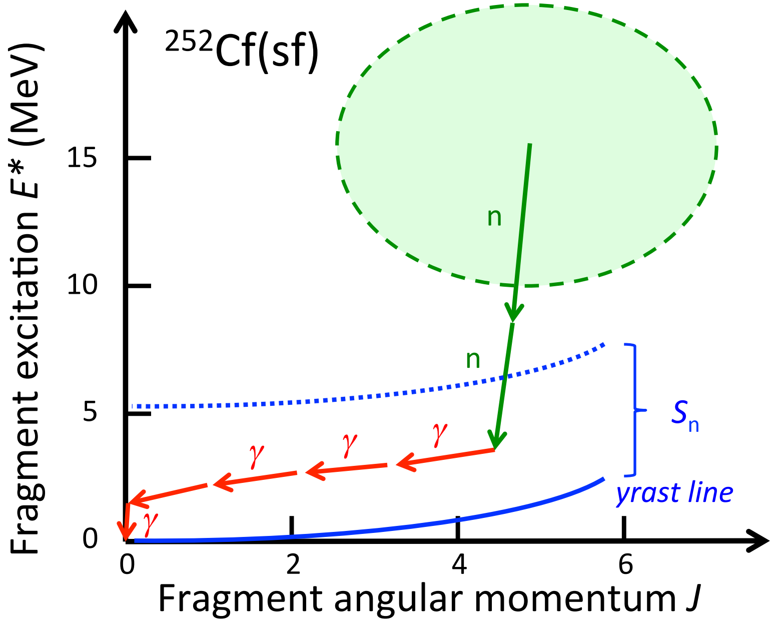

.. then by stretched E2 photons along the yrast line …

$$S_f = S_i - 2$$
$$\epsilon_\gamma = S_i^2/2\mathcal{I}_A - S_f^2/2\mathcal{I}_A$$
$$\mathcal{I}_A = 0.5 \times \tfrac{2}{5} A m_N R_A^2$$

… whenever possible, the RIPL decay tables are used instead…

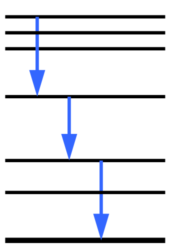

Each photon is Lorentz boosted from the emitter to the laboratory frame

Fragment spin and photon emission are correlated

- Photon multiplicity from both fragments increases fairly linearly with combined fragment spin for $S_L + S_H > 5\hbar$
- Behavior is independent of E_n and of fissioning system
- Slope depends on multiplier of rigid body moment of inertia, usually 0.5, but a smaller factor, like 0.3, would lead to a steeper increase
- Photon multiplicity can then be used as a proxy for total fragment spin

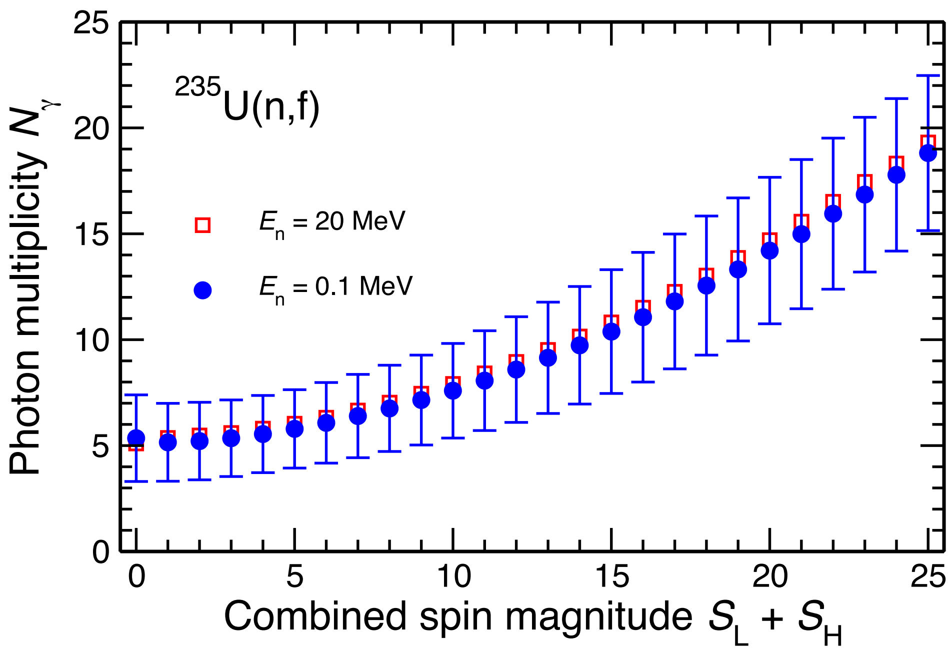

R.V. and J. Randrup, PRC, submitted

Dominance of fluctuations results in very weak fragment spin correlation

- The fragment spins $\boldsymbol{S}_L$ & $\boldsymbol{S}_H$ are dominated by wriggling & bending fluctuations and are only very weakly correlated (both mutually and w.r.t $\boldsymbol{S}_0$)
- Recoil from wriggling creates some orbital motion and the subsequent Coulomb trajectory reorients the direction of the relative fragment motion by about 2°
- The remaining weak directional correlation is effectively independent of the initial energy, the compound nuclear spin, and the fragment mass division
- There is a slight preference for opposite spin directions: $P(180°)/P(0°) = 1.18$

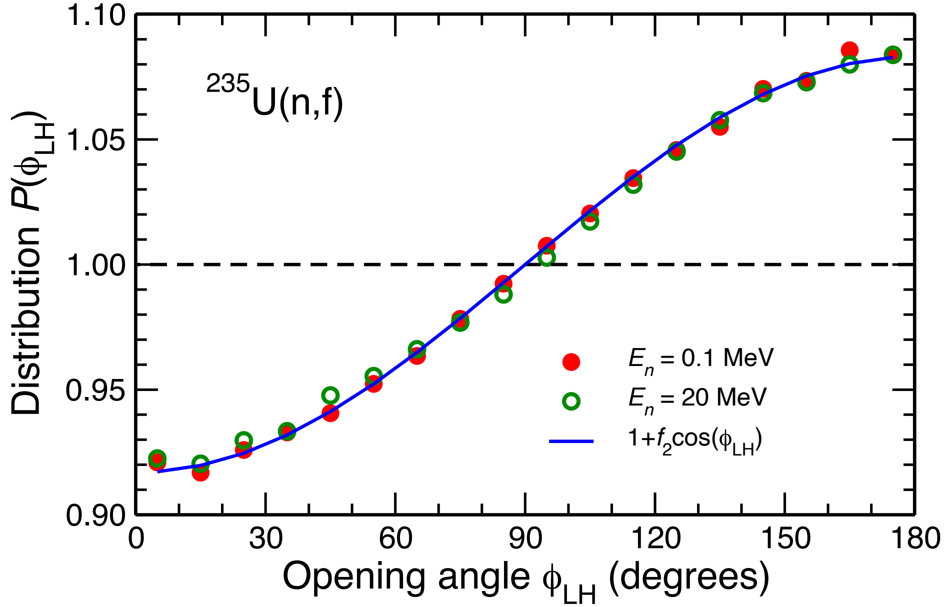

R.V. and J. Randrup, PRC, submitted

Neutron emission from rotating fragments causes angular anisotropy

- Neutron emission from a rotating fragment results in an equatorial bulge in the angular distribution due to centrifugal force
- The bulge is practically independent of the initial compound spin
- The resulting *dynamical anisotropy* can be expressed by
  $A = dN_n/d\Omega_{nS}(90^o)/dN_n/d\Omega_{nS}(0) - 1 = 0.093$
- The evaporation chains reorient the fragment spins by 13^o on average but change the spin magnitudes only slightly, by $0.06\hbar$

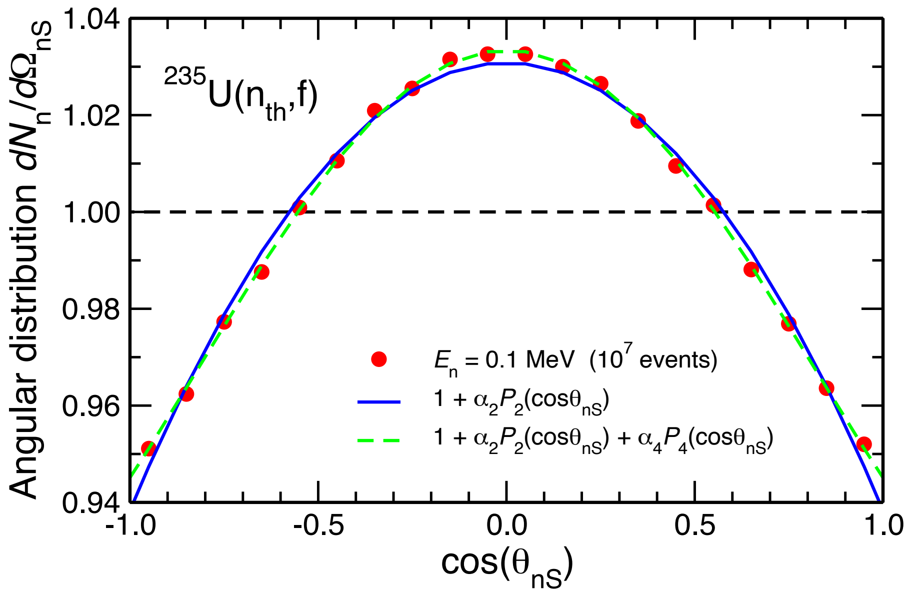

R.V. and J. Randrup, PRC, submitted

Neutron velocity distribution from $^{235}U(n_{th},f)$

- Combined neutron velocity distributions from the two fragments
- The circles show neutron kinetic energies of 1 MeV (solid) and 2 MeV (dashed)

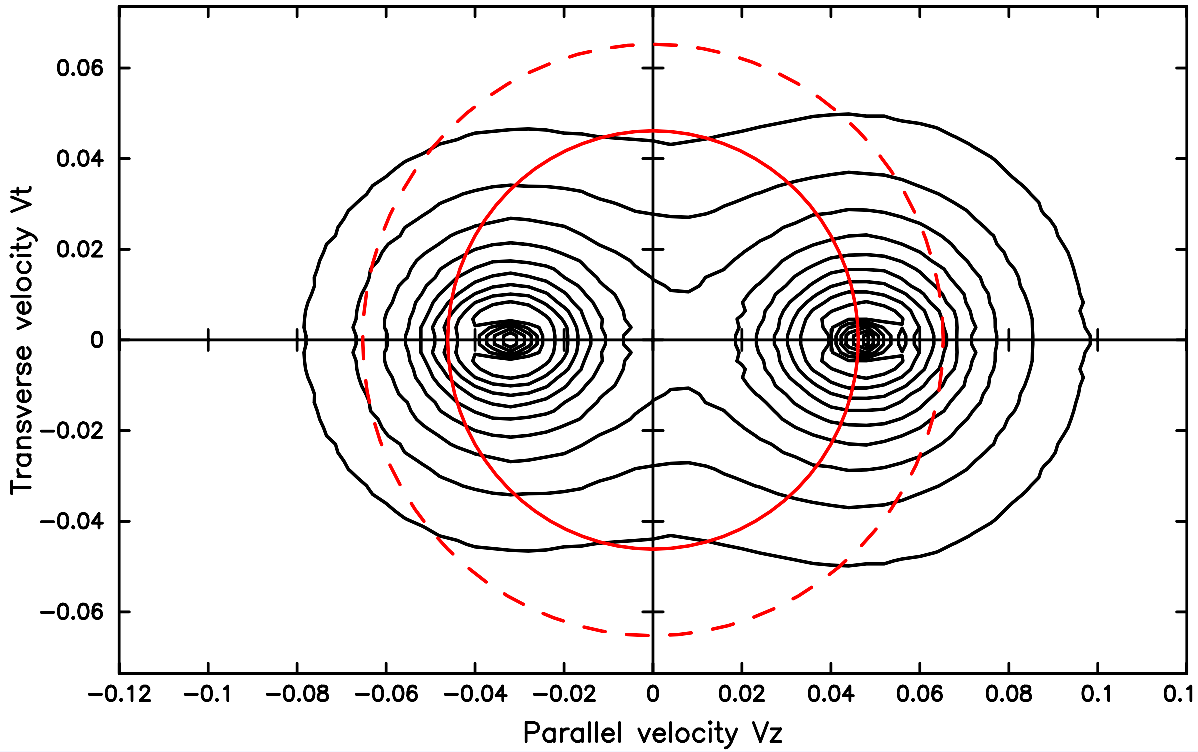

R.V. and J. Randrup, PRC, submitted

Neutron distribution relative to light fragment direction

- Neutron distributions are forward-backward asymmetric with respect to light fragment because the light fragment has a higher velocity and emits more neutrons
- It becomes more strongly asymmetric for higher neutron kinetic energies and more symmetric for low energy neutrons
- Almost no dependence on rotational boost

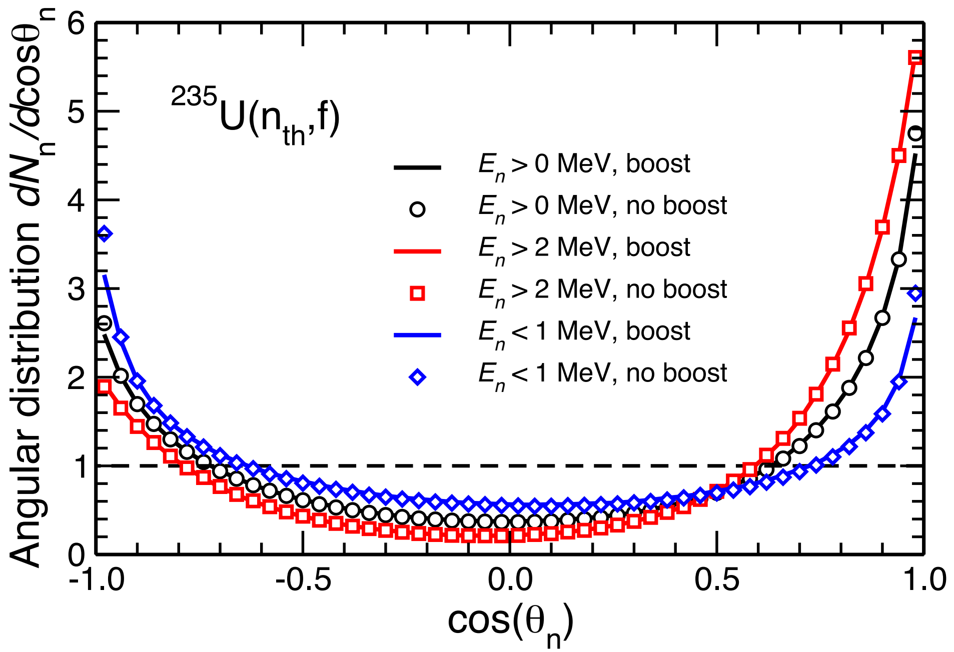

R.V. and J. Randrup, PRC, submitted

Two-neutron correlations show effect of F-B asymmetry, less dependence on total fragment spin

Low energy neutrons are more likely to be less correlated, more isotropic, at small angles

Higher energy neutrons exhibit the typical two-peak correlation

Little correlation with low or high total fragment spin

Similar behavior seen when, instead of spin, correlation is with photon multiplicity

Differences in correlation with N_γ may be because higher photon multiplicity is associated with fewer or less energetic neutrons

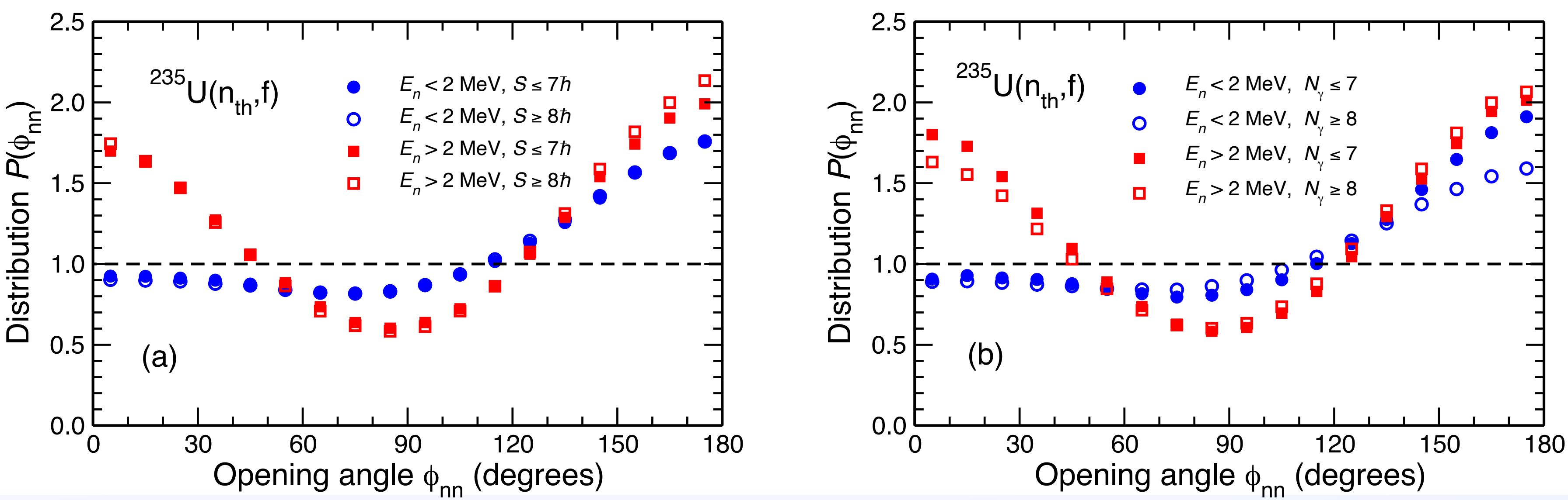

R.V. and J. Randrup, PRC, submitted

We can look for more direct spin effects in nature

- ^{235}U has spin 7/2 in its ground state, so $^{235}U(n,f)$ leads to the compound nucleus $^{236}U^*$ with spin $3\hbar$ or $4\hbar$
- ^{235}U also has a spin 1/2 isomeric state with a 26-minute half life, leading to a compound nucleus $^{236}U^*$ with spin 0 or $1\hbar$
- Does this difference in initial spin have observable consequences?

Nuclide	Energy [keV]	J^π	$T_{1/2}$ Abund. [mole fract.]
$^{235}_{92}U_{143}$	0.0	7/2-	7.04×10^8 y 1 **0.7204 % 6**
$^{235m1}_{92}U_{143}$	0.0760 4	1/2+	26 min

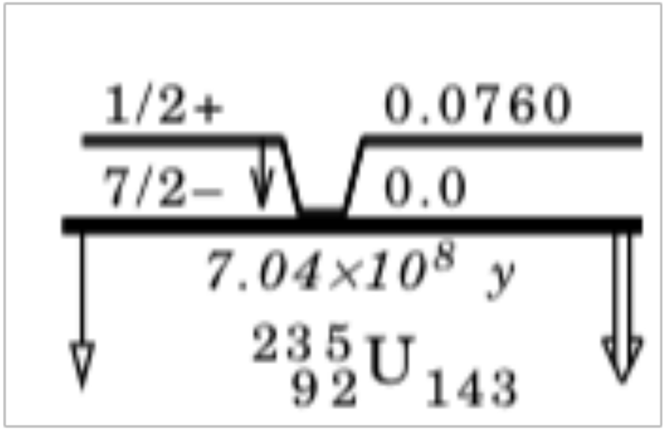

Thermal fission with spin zero could change yields

- Thermal fission for spin zero could enhance the symmetric yields by 5% due to pairing effects in the barrier region (shown for $^{234}U^*$ but the results are similar for $^{236}U^*$)
- Based on this premise, we have constructed a *Y*(*A*) for input to FREYA with a 5% enhanced symmetric yield (and consequent reduction of the peak yields)
- We then look for observable consequences of these changed yields

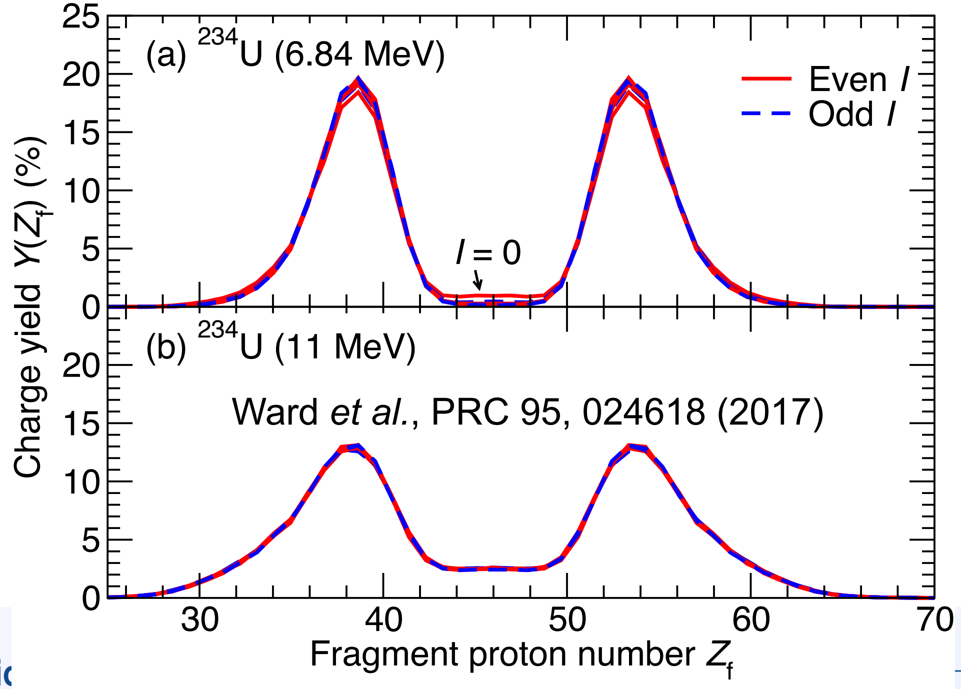

Observable consequences of fission from the isomeric state

- The enhanced symmetric yield results in higher neutron multiplicities at low TKE
- These neutrons show up in the high-energy tail of the multiplicity distribution, only slightly affecting the multiplicity moments; such modifications could be observable if isomeric targets could be made and sufficient statistics gathered

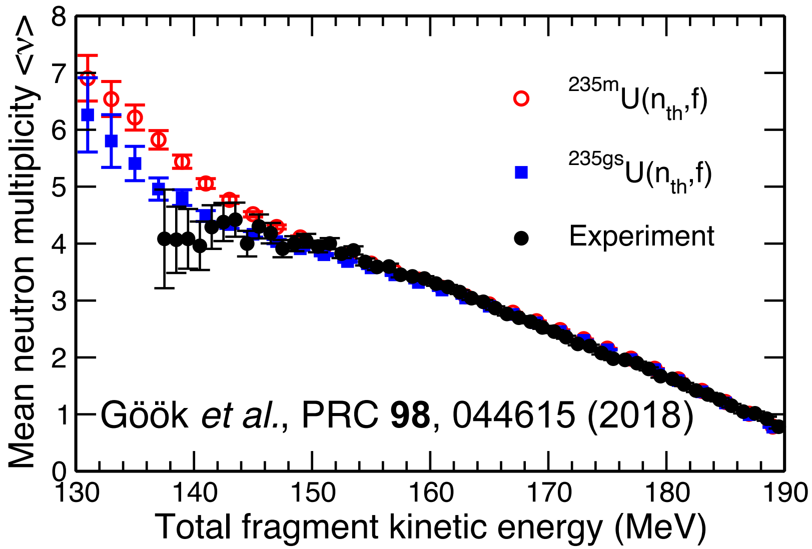

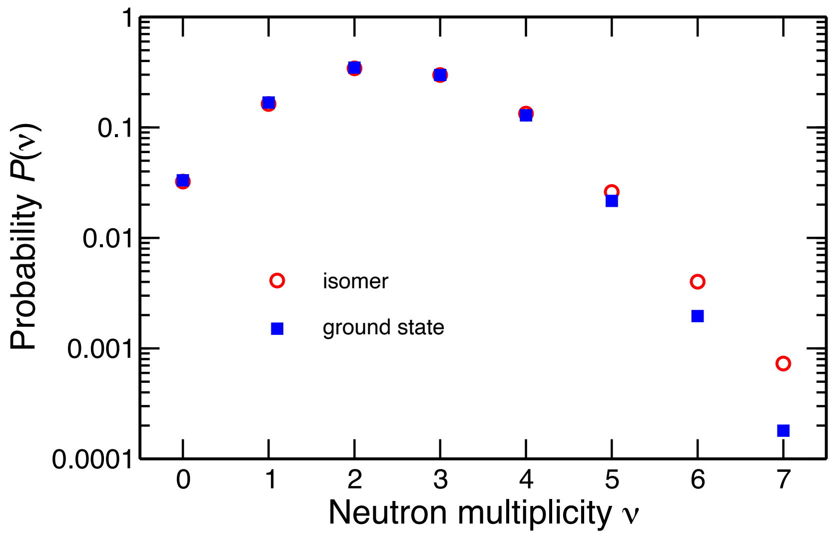

Neutron multiplicity moments

Case	M1	M2	M3	M4
$^{235gs}U(n_{th},f)$, $S_0=4\hbar$	2.39526	4.53167	6.46183	6.59926
$^{235m}U(n_{th},f)$, $S_0=0$	2.43591	4.75387	7.23551	8.6252

R.V. and J. Randrup, PRC, submitted

FREYA can be applied to test results of microscopic calculations

- Nicolas Schunck and Petar Marevic provided spin distributions for heavy fragments from fission of ^{240}Pu:
  - $A_H = 122$, $Z_H = 48$
  - $A_H = 140$, $Z_H = 54$
  - $A_H = 150$, $Z_H = 58$
- As a first test, we can extract spin distributions from FREYA for the same A_H/A_L splits with our default parameter and compare them directly
- To see the consequences of the microscopically-calculated spin distributions, we can modify our parameter c_S to obtain spin distributions that match their calculations
- With the modified distributions, we can look for consequences of these new spin distributions on neutron and photon observables

FREYA default P(J) compared to microscopic P(J)

- The microscopic distributions tend to be much broader or “hotter” than the standard FREYA result with a significantly higher spin

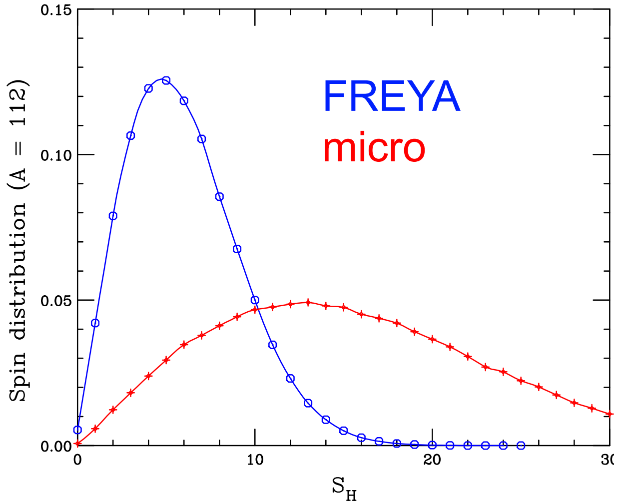

$A_H = 122$
$S_H(\text{FREYA}) = 6.79\hbar$
$S_H(\text{micro}) = 17.39\hbar$

$A_H = 140$
$S_H(\text{FREYA}) = 6.64\hbar$
$S_H(\text{micro}) = 11.46\hbar$

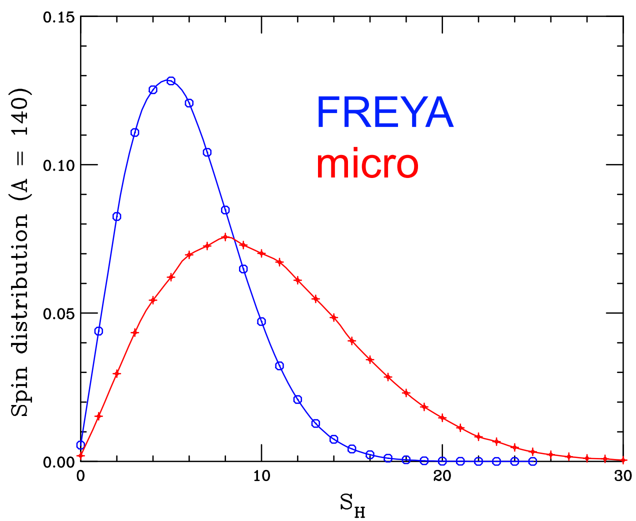

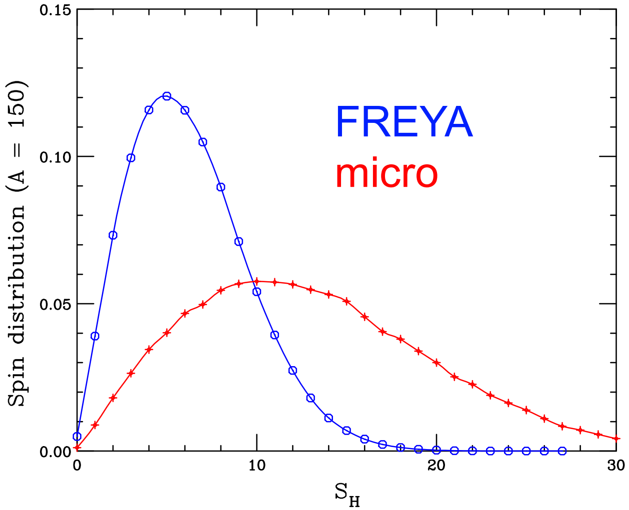

$A_H = 150$
$S_H(\text{FREYA}) = 7.03\hbar$
$S_H(\text{micro}) = 14.71\hbar$

Higher average spin significantly affects neutron and photon emission

- Giving the heavy fragment more spin reduces neutron emission and increases photon emission for the three heavy fragments chosen.

Model	c_S	Mass split	S_H ($\hbar$)	ν_H	ν	N_γ
FREYA	0.87	all	6.70	1.15	2.88	8.20
FREYA	0.87	122/118	6.79	1.76	4.31	10.36
micro	7.0	122/118	17.39	1.15	2.90	26.57
FREYA	0.87	140/100	6.64	1.37	2.90	7.54
micro	3.0	140/100	11.46	1.13	2.42	13.10
FREYA	0.87	150/90	7.03	1.61	2.91	9.40
micro	4.5	150/90	14.71	1.16	2.10	18.99

Summary

- Studies with FREYA show there is only a weak correlation between the fragment spins
- We confirm there exists a dynamical anisotropy due to neutron emission from spinning fragments but no strong dependence on the initial spin
- Relative to ^{235gs}U(n,f), the isomeric reaction ^{235m}U(n,f), enhances the symmetric mass yields which in turn could lead to enhanced neutron emission at low fragment total kinetic energy
- FREYA is a useful tool for testing how results from microscopic models affect observables

Rotational modes of a dinucleus

After scission, fragments rotate around axis between their centers (rigid rotation) but their relative motion can also fluctuate (wriggling, bending, tilting and twisting modes)

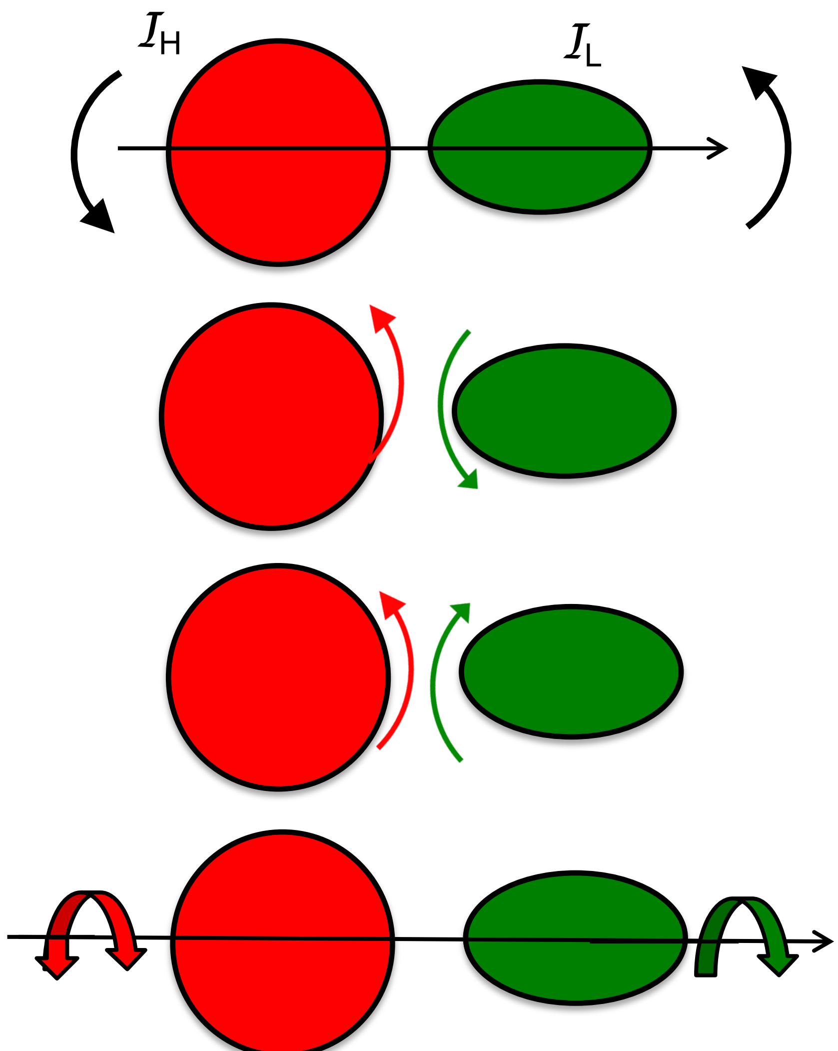

Rigid rotation:

Wriggling (2):

Bending (2):

Tilting & twisting:

Moments of Inertia:

$\mathcal{J}_{\mathrm{tot}} = \mathcal{J}_{\mathrm{L}} + \mathcal{J}_{\mathrm{H}} + \mathcal{J}_{\mathrm{rel}}$

$\mathcal{J}_{\mathrm{rel}} = \mu R^2$

$R = R_{\mathrm{L}} - R_{\mathrm{H}}$;
$\mu = m_N A_{\mathrm{L}} A_{\mathrm{H}} / (A_{\mathrm{L}} + A_{\mathrm{H}})$

$\mathcal{J}_{\mathrm{L}} = (1/2)(M_L R_L^2/5)$

$\mathcal{J}_{\mathrm{H}} = (1/2)(M_H R_H^2/5)$

$\mathcal{J}_{+} = (\mathcal{J}_{\mathrm{H}} + \mathcal{J}_{\mathrm{L}})\mathcal{J}/\mathcal{J}_{\mathrm{rel}}$

$\mathcal{J}_{-} = \mathcal{J}_{\mathrm{H}}\mathcal{J}_{\mathrm{L}}/(\mathcal{J}_{\mathrm{H}} + \mathcal{J}_{\mathrm{L}})$

$\mathcal{J}_{\mathrm{H}} + \mathcal{J}_{\mathrm{L}}$ IGNORED!